

Edge-mode velocities and thermal coherence of quantum Hall interferometers

Zi-Xiang Hu,¹ E. H. Rezayi,² Xin Wan,^{1,3,4} and Kun Yang⁵

¹*Asia Pacific Center for Theoretical Physics, Pohang, Gyeongbuk 790-784, Korea*

²*Department of Physics, California State University Los Angeles, Los Angeles, California 90032, USA*

³*Department of Physics, Pohang University of Science and Technology, Pohang, Gyeongbuk 790-784, Korea*

⁴*Zhejiang Institute of Modern Physics, Zhejiang University, Hangzhou 310027, P.R. China*

⁵*National High Magnetic Field Laboratory and Department of Physics,*

Florida State University, Tallahassee, Florida 32306, USA

(Dated: May 30, 2018)

We present comprehensive results on the edge-mode velocities in a quantum Hall droplet with realistic interaction and confinement at various filling fractions. We demonstrate that the charge-mode velocity scales roughly with the valence Landau level filling fraction and the Coulomb energy in the corresponding Landau level. At Landau level filling fraction $\nu = 5/2$, the stark difference between the bosonic charge-mode velocity and the fermionic neutral-mode velocity can manifest itself in the thermal smearing of the non-Abelian quasiparticle interference. We estimate the dependence of the coherence temperature on the confining potential strength, which may be tunable experimentally to enhance the non-Abelian state.

I. INTRODUCTION

Fractional quantum Hall (FQH) states are incompressible quantum liquids that support fractionalized quasiparticles and gapless edge excitations¹. The simplest edge theory for the Laughlin states contains a single branch of charge mode, which is described by chiral bosons². The velocity of the charged bosons v_c , which enters the effective theory through gauge-fixing condition, depends on electron-electron interaction and edge confinement in general and is, therefore, not a universal quantity. Recent development of quantum Hall interferometers^{3,4} also allows experimental determination of v_c from current oscillations in the devices.

Apart from the charge mode, which seems to dominate the edge tunneling measurement,⁵ neutral edge modes may arise in the hierarchical states^{6,7,8} or through edge reconstruction.^{9,10,11,12,13} The velocities of the neutral modes v_n , which no experiments have observed, are conceivably smaller than v_c ^{14,15}. At Landau level (LL) filling fraction $\nu = 5/2$,^{16,17,18} a neutral Majorana fermion mode exists in the Moore-Read phase. In the non-Abelian FQH state, numerical studies^{19,20} found v_n to be roughly 10 times smaller than v_c in a model with long-range interaction and confining potential due to neutralizing background charge. Even smaller v_n/v_c has been proposed to explain tunneling conductance measurement at $\nu = 2/5$.²¹

The stark difference in the edge-mode velocities in the Moore-Read phase can lead to “Bose-Fermi separation”,²⁰ which resembles spin-charge separation in Luttinger liquids. When propagating along the edge, quasiparticles with charge $e/4$ carrying both charged bosonic and neutral fermionic components smear at finite temperatures. This poses a stringent requirement on the observation of current oscillations due to quasiparticle interference in a double point-contact interferometer,^{22,23,24,25,26} whose contact distance should not exceed the quasiparticle dephasing length.²⁷ On the other hand, the Abelian charge $e/2$ quasiparticles carrying the bosonic component *only* (and thus not affected by the slow fermionic mode) smear significantly less and may dominate the current

oscillations at higher temperatures when charge $e/4$ quasiparticle transport is incoherent,²⁰ even though the tunneling amplitude of the charge $e/2$ quasiparticles is much smaller than that of the charge $e/4$ quasiparticles.^{28,29}

Recently, experimentalists observed³⁰ conductance oscillations consistent with the interference of both $e/4$ and $e/2$ quasiparticles in a double point contact interferometer at $\nu = 5/2$, and the dominance of $e/2$ periods at higher temperatures when the conductance oscillations are still visible. Further observation of the alternative $e/4$ and $e/2$ oscillations³¹ is now under examinations²⁹ on its potential origin in the odd-even effect^{25,26} due to non-Abelian statistics, mingled with the bulk-edge coupling effect.^{32,33,34} The interpretation of the experimental findings as non-Abelian interference²⁹ (as opposed to, e.g., the charging effect^{35,36,37}) relies crucially on the estimate of edge-mode velocities from numerical studies,²⁰ which predicted significant difference in coherent lengths or coherent temperatures for charge $e/4$ and $e/2$ quasiparticles.

In this paper, we report results on studies of edge-mode velocities in a realistic microscopic model for both Abelian and non-Abelian FQH liquids, including the analysis on finite-size effect and the effect of edge confinement. We show that the charge-mode velocity v_c is roughly proportional to the valence LL filling fraction and the Coulomb energy scale in the corresponding LL, while the neutral-mode velocity v_n in the Moore-Read phase is consistently smaller. We further present our estimate of the coherent temperatures for charge $e/4$ and $e/2$ quasiparticles in the Moore-Read phase based on the quantitative knowledge of the two velocities, and show that they are in quantitative agreement with recent experiments.

The rest of the paper is organized as follows. We introduce our model and discuss its relevance to an experimental setup in Sec. II. We present our main results on edge-mode velocities in Sec. III and discuss their implication on interference experiments in Sec. IV. We discuss the limitation of our microscopic approach and summarize the paper in Sec. V.

II. GROUNDSTABILITY IN A CHARGE-NEUTRAL MODEL

We consider a microscopic model of a two-dimensional electron gas (2DEG) in a disk geometry with long-range Coulomb interaction among electrons in the lowest Landau level (0LL) or the first excited Landau level (1LL). We introduce a confining potential by including neutralizing background charge distributed uniformly on a parallel disk at a distance d from the 2DEG. The model prototypes a modulation-doped sample, which separates charged impurities spatially from the electron layer for high charge mobility. We use the location of the background charge to tune from stronger confinement (smaller d) to weaker confinement (larger d). The microscopic Hamiltonian is

$$H_C = \frac{1}{2} \sum_{mnl} V_{mn}^l c_{m+l}^\dagger c_n^\dagger c_{n+l} c_m + \sum_m U_m c_m^\dagger c_m, \quad (1)$$

where c_m^\dagger creates an electron in a single-particle state with angular momentum m in the symmetric gauge. V_{mn}^l 's are the corresponding matrix elements of Coulomb interaction, and U_m 's the matrix elements of the confining potential.^{12,20} The definitions of the electron operators and matrix elements are consistent with the corresponding LL index; the common practice is to map them into the 0LL representation using ladder operators across LLs.³⁸ At various ν , we study the spectrum of the model Hamiltonian numerically by exact diagonalization using the Lanczos algorithm up to 7 electrons for $\nu = 1/5$, 10 electrons for $\nu = 1/3$, 14 electrons for $\nu = 5/2$, and 20 electrons for $\nu = 2/3$.

Our approach features the inclusion of a realistic confining potential due to the neutralizing background charge; it allows us to study the energetics in the microscopic model quantitatively and compare with the experimental observations. For example, we can identify various phases by studying the total angular momentum of the ground state M_{gs} of the model as d varies at a given ν , as illustrated in Fig. 1. In Fig. 1(a), we plot the ground state energy $E(M)$ in each total angular momentum (M) subspace for $N = 12$ electrons in 22 1LL orbitals, i.e. at $\nu = 5/2$. When the background charge lies at $d/l_B = 0.4, 0.6,$ and 0.8 , M_{gs} yields 121, 126, and 136, respectively. The global ground state at $d = 0.6l_B$ has the same M_{gs} as that of the $N = 12$ Moore-Read state $M_{\text{MR}} = N(2N - 3)/2 = 126$; thus we say that the Moore-Read state is *groundstable*³⁹ at $d = 0.6l_B$. Our calculation shows that the 12-electron Moore-Read state is groundstable in 22 1LL orbitals with $0.51 \leq (d/l_B) \leq 0.76$, as indicated in Fig. 1(b). We have shown that the ground state evolves continuously into the Moore-Read state when the Coulomb interaction changes smoothly to a three-body interaction in Ref. 20, which also discussed the nature of the other ground states.

Our main motivation to introduce a neutralizing charge background at a distance d away from the 2DEG is for modeling experimental structures. In ultra-high-mobility GaAs samples,⁴⁰ an undoped setback, whose thickness optimizes charge mobility, separates a thin layer of Si impurities and the 2DEG. Therefore, it is tempting to identify d in our model as (or to

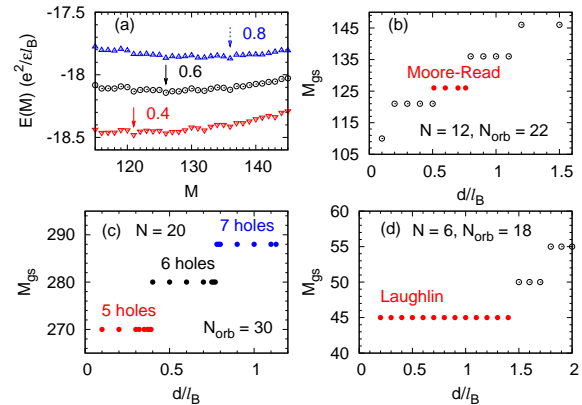


FIG. 1: (color online) (a) Ground state energy $E(M)$ in each total angular momentum M subspace for $N = 12$ electrons with 22 orbitals in the 1LL ($\nu = 5/2$). The neutralizing background charge is at a distance $d/l_B = 0.4, 0.6,$ and 0.8 away from the 2DEG. The total angular momentum of the global ground state M_{gs} (indicated by arrows) increases from 121, 126, to 136, respectively. The global ground state at $d = 0.6l_B$ has the same total angular momentum $M_{\text{MR}} = N(2N - 3)/2 = 126$ as the corresponding $N = 12$ Moore-Read state. We have shifted the curves vertically for $d = 0.4l_B$ and $0.8l_B$ for clarity. (b) M_{gs} as a function of d at $\nu = 5/2$. The solid dots indicate the plateau at which the Moore-Read state is groundstable. (c) M_{gs} as a function of d for 20 electrons in 30 orbitals ($\nu = 2/3$). We can understand the three plateaus of M_{gs} as $\nu = 1/3$ Laughlin droplets of 5-7 holes embedded in a $\nu = 1$ electron droplet. Note that they are in the same phase, but the corresponding distances between two counterpropagating edges are different.⁸ (d) M_{gs} as a function of d for 6 electrons in 18 orbitals ($\nu = 1/3$). The solid dots indicate the plateau at which the Laughlin state is groundstable. Beyond $d \approx 1.5l_B$, the system undergoes an edge-reconstruction transition.^{10,12}

quantitatively relate it to) the thickness of the setback layer, which can be of the order of 1000 \AA ,⁴¹ or about 10 magnetic length l_B for a typical magnetic field strength ($\sim 5 \text{ T}$, as in Ref. 30). However, the direct identification is an oversimplification. In past studies, we have encountered at least three different scenarios in which additional edges are present in the system and spoil the identification by changing the effective edge confining potential. First, as in the $\nu = 5/2$ case,²⁰ filled LLs introduce integer edges, which may influence the confining potential of the inner edge for the partially filled LL. Second, in a nonchiral case like $\nu = 2/3$,⁸ two counterpropagating edges can move relatively to each other to adjust their shares of the confining potential, leading to a series of ground states with different M_{gs} , as illustrated in Fig. 1(c). Nevertheless, they belong to the same phase.⁸ Finally, even in the case of a single chiral edge, a fractional quantum Hall droplet may undergo one or more edge-reconstruction transitions to introduce counterpropagating edges for $d > 1.5l_B$ [as illustrated in Fig. 1(d)], beyond which the microscopic calculation suffers from size limitation.¹² However, even with the complications, we believe that the introduction of d is experimentally relevant in the following two ways. First, the range of d in which a specific phase is groundstable often indicates the

stability of the phase, as the comparison of Figs. 1(b) and 1(d) clearly demonstrates. Second, the relative value of d measures the relative strength of the confining potential, thus allowing qualitative and, sometimes, quantitative predictions from the model calculation.

III. EDGE-MODE VELOCITIES

At $\nu = 1/3$, the edge excitations arise from a single branch of bosonic charge mode as illustrated in Fig. 2(a) for $N = 8$ electrons and $d = 0.6l_B$. Ref. 12, in the context of edge reconstruction, has explained in detail the method for the identification of the edge excitations among all excitations. In a finite system, we can then define v_c through (i) the excitation energy $\Delta E(\Delta M = 1)$ of the smallest momentum mode with edge momentum $k = \Delta M/R = 1/R$, i.e. $v_c^\Delta = (R/\hbar)\Delta E(\Delta M = 1)$, where $R = \sqrt{2N/\nu}$ is the radius of the droplet, or (ii) the slope at $k = 0$ of the dispersion curve [see Fig. 2(b)] fitted to the edge-mode energies, i.e. $v_c^d = (R/\hbar)(dE/dM)$. As shown in Fig. 2(c), both definitions point to $\sim 0.3e^2/\epsilon\hbar$ in the thermodynamic limit and are therefore suitable. The definition v_c^d is less robust due to the nonlinear dispersion at small k in finite systems; thus, we will use the definition v_c^Δ in later analyses. In general, v_c depends on the strength of the confining potential, which is determined by *charge neutrality* and is meaningful only when the Laughlin variational wavefunction is *ground-stable*,³⁹ i.e. the Coulomb ground state has the same angular momentum as the Laughlin state. For $\nu = 1/3$, neutrality limits v_c from above, while groundstability from below,^{10,12} allowing v_c to vary between $0.21\sim 0.40e^2/\epsilon\hbar$ (see Fig. 3), or $3.5\sim 6.7 \times 10^6$ cm/s in GaAs systems (with dielectric constant $\epsilon \approx 13$). A similar analysis for $\nu = 1/5$ (with less robust finite-size analysis due to computational limitation) reveals v_c to be $0.20\sim 0.26e^2/\epsilon\hbar$, or $3.4\sim 4.4 \times 10^6$ cm/s for GaAs.

We now turn to $\nu = 5/2$, or a valence LL filling $\nu^* = \nu - \lfloor \nu \rfloor = 1/2$, after subtracting the filled OLL. The even-denominator quantum Hall state is widely expected to be the Moore-Read Pfaffian state,¹⁶ described by the $SU(2)_2$ topological quantum field theory, or its particle-hole conjugate, the anti-Pfaffian state.^{17,18} In numerical studies, the Pfaffian state can be stabilized on the disk geometry,^{19,20} whose edge contains both neutral Majorana fermions and charged chiral bosons. The heavy mixture of the bulk and edge excitations complicates the extraction of $v_{c,n}$.¹⁹ Therefore, we mix the 3-body interaction with the Coulomb interaction to separate the edge and bulk excitations in energy and extrapolate the calculated velocities to the pure Coulomb case.²⁰ Based on a similar finite-size scaling in systems of 6-14 electrons as described above, we obtain $0.36e^2/\epsilon\hbar < v_c < 0.38e^2/\epsilon\hbar$, or $6 \times 10^6 < v_c < 6.4 \times 10^6$ cm/s for GaAs, which is about 20% larger than the estimate based on a 12-electron system.²⁰

We summarize the range of v_c in Fig. 3. For $\nu = 2/3$, we include both the left- and right-going-mode velocities,^{42,8} arising from the coupling of the edge modes^{1,7} of the inner Laughlin $\nu = 1/3$ hole droplet and the outer $\nu = 1$ droplet^{6,43}. Since the Coulomb energy is the only energy scale, dimen-

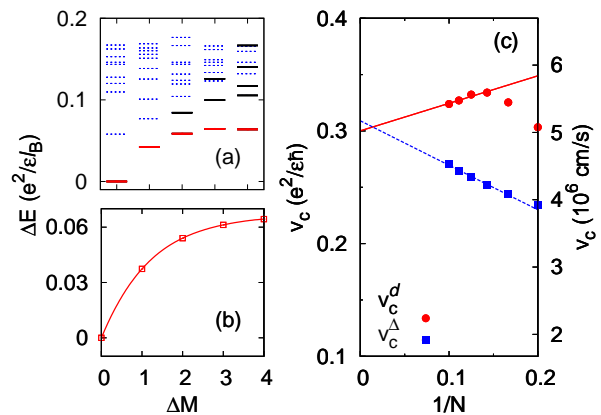


FIG. 2: (color online) Edge-mode velocity analysis for $\nu = 1/3$. (a) Low-energy excitations in a $N = 8$ system with background charge at $d = 0.6l_B$, with edge excitations marked by solid bars. (b) Energies of single chiral boson excitations, which are the ground states in individual momentum spaces [marked in red in (a)]. (c) Chiral boson (or charge mode) velocity v_c defined either by the slope of the best quadratic fit in (b) at the origin (v_c^d) or by the ground-state energy difference at $\Delta M = 0$ and 1 (v_c^Δ) for systems of 5-10 electrons. The finite-size scaling of v_c^Δ shows a weaker nonlinear effect, although the two definitions tend to give the same result in the thermodynamic limit.

sional analysis implies

$$v_c \sim \nu^* e^2/\epsilon\hbar = (\nu^* \alpha/\epsilon)c, \quad (2)$$

where c is the speed of light in vacuum and $\alpha \approx 1/137$ the fine-structure constant. Our numerical results, including the larger velocity for $\nu = 2/3$ (which we assume to be the charge-mode velocity), agrees well with Eq. (2). At $\nu = 5/2$, we can attribute the deviation to the reduction of the Coulomb energy scale in the 1LL, due to the change of the LL structure factor. On the other hand, the counterpropagating (presumably neutral) mode at $\nu = 2/3$ has a velocity closer to the value for $\nu = 1/3$; in finite systems, we cannot resolve whether the interedge Coulomb coupling (divergent in the long wavelength limit) can lower the value (as being decoupled from charge, the neutral mode has a conceivably small velocity). Recently, trial wavefunctions are under consideration for such FQH states with negative flux in the composite fermion approach.⁴⁴ It is worth mentioning that the results of v_c are consistent with the recent experimental determinations of v_c to be 4×10^6 cm/s for $\nu = 1/3$ ³ or to saturate at 1.5×10^7 cm/s in the integer regime,⁴ further justifying the validity of our microscopic model calculation. They are also quantitatively consistent with earlier time-resolved transport measurements.^{45,46,47}

On the other hand, theoretical proposals agree on a smaller value for v_n , with electrostatic,¹⁴ topological,¹⁵ and dynamic origins.⁴⁸ But the edge magnetoplasmon experiment in the time domain,⁴⁵ e.g., showed no hint of the existence of a counterpropagating edge mode at $\nu = 2/3$, although theories^{1,6,7,43} and the numerical study on a realistic model⁸ suggested its existence. In the chiral case at $\nu = 5/2$, we found

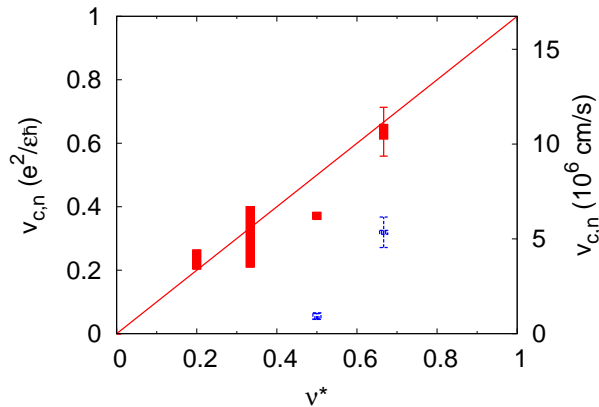


FIG. 3: (color online) Summary of the charge-mode velocity v_c (solid red candles) and neutral-mode velocity v_n (empty blue candles), extrapolated to the thermodynamic limit (except for $\nu = 2/3$), at various valence LL filling $\nu^* = \nu - \lfloor \nu \rfloor$. The size of the candles reflects the range of velocities in the corresponding groundstate range of the confining potential strength (or d). The candle data for $\nu = 2/3$ are based on 20 electrons in 30 orbitals for various confining potential strength, while the errorbars reflect our estimate of the uncertainty due to finite-size effects. The solid line is the dimensional analysis result $v_c = \nu^* e^2 / \epsilon \hbar$.

v_n to be one order of magnitude smaller than v_c in a system with $N = 12$ electrons at $d = 0.6l_B$.²⁰ Here, we extend the study on v_n by exploring the parameter space of d and N , as long as the Moore-Read phase is the stable ground state, or *groundstateable*, with Coulomb interaction among electrons. As explained in earlier studies,²⁰ we first mix 3-body interaction with Coulomb interaction to allow a clear separation of bulk modes and edge modes. In this case, the lowest edge excitation with $\Delta M = 2$ has an excitation energy ΔE_n being the sum of the two neutral excitation energies at $kR = 1/2$ and $3/2$ due to the anti-periodic boundary condition in the absence of bulk quasiparticles. Therefore, we expect $v_n = (R/2\hbar)\Delta E_n(\Delta M = 2)$. Extrapolating data to the pure Coulomb case and to the thermodynamic limit, we obtain the range of v_n to be $0.045 \sim 0.065 e^2 / \epsilon \hbar$, or $0.75 \sim 1.1 \times 10^6$ cm/s for GaAs. The finite-size scaling analysis reveals that the value of v_n in a 12-electron system obtained earlier²⁰ is about 40% smaller than its thermodynamic value, though we still have a large ratio $v_c/v_n \approx 6 \sim 8$.

Within the groundstateable range of the parameter space, the velocities decrease as d increases, i.e., as the confining potential strength becomes weaker. We can fit the trend by a linear dependence on d . At $\nu = 5/2$, we find that the velocities in the thermodynamic limit are

$$v_c = 0.435 - 0.106d/l_B \quad (3)$$

$$v_n = 0.123 - 0.120d/l_B, \quad (4)$$

in unit of $e^2 / \epsilon \hbar$.

IV. THERMAL DECOHERENCE IN INTERFERENCE EXPERIMENTS

The small v_n , as opposed to the larger v_c , dominates the thermal smearing of the non-Abelian $e/4$ quasiparticles in edge transport. In an interference experiment, finite temperature T introduces an additional energy scale to compete with the traverse frequency for quasiparticles (or edge waves) propagating from one point contact to another between multiple reflections within the interferometer. Therefore, the Aharonov-Bohm type oscillation will be washed out above the coherence temperature²⁹

$$T^* = \frac{1}{2\pi L k_B} \left(\frac{g_c}{v_c} + \frac{g_n}{v_n} \right)^{-1}, \quad (5)$$

where L is the distance along the interference path between the two point contacts. For the Moore-Read Pfaffian (or anti-Pfaffian) state, $g_c = 1/8$ and $g_n = 1/8$ (or $3/8$) are the corresponding scaling dimensions. Using our results for v_c and v_n , we plot T^* in the Moore-Read phase for charge $e/4$ quasiparticles and the $e/2$ quasiparticles in the Ising vacuum sector ($g_c = 1/2$ and $g_n = 0$) as a function of d in Fig. 4, assuming a point contact distance of $L = 1 \mu\text{m}$. Here, we use the extrapolated value of v_c and v_n in the thermodynamic limit for the Coulomb interaction [Eqs. (3) and (4)]. Therefore, in an interference experiment, we expect that with increasing T the conductance oscillations due to the interference of $e/4$ quasiparticles (thus signatures of non-Abelian statistics) will disappear first at a lower temperature, which depends strongly on the details of the confinement potential. On the other hand, the oscillations due to $e/2$ quasiparticles will persist up to about 150 mK, which is less sensitive to the confinement. This picture and the corresponding temperature ranges agree with the Willett experiment³⁰ quantitatively.

For the solid range of the curves in Fig. 4 (or $0.47 \leq d/l_B \leq 0.62$), we can justify the groundstateability of the Moore-Read state in a 12-electron system in 26 orbitals with the pure Coulomb interaction. This range is sensitive to the system size and the number of orbitals; e.g., we found it to be $0.51 \leq d/l_B \leq 0.76$ for the 12-electron system in 22 orbitals. This indicates that the stability of the Moore-Read state is sensitive to the sharpness of the edge confinement. In general, we find the groundstateable range becomes wider in larger systems; therefore, it is tempting to extrapolate the trend in velocities [Eqs. (3) and (4)] to $d_c \approx l_B$, where v_n vanishes. However, a potentially competing stripe phase may arise below d_c .²⁰ Accordingly, we extrapolate the coherence temperatures further in weaker confinement, as illustrated by the broken lines in Fig. 4.

One can probe the sensitive dependence of T^* on d for $e/4$ quasiparticles by controlling l_B via tuning electron density and magnetic field simultaneously or by applying an external confining potential. This would indirectly support our conclusion that it is the smallness of v_n that controls the coherence length or temperature. Direct evidence may come from the transport measurements of a long tunneling contact⁴⁹ or from the momentum-resolved tunneling measurements,^{50,51} in which the slower neutral mode is accessible.

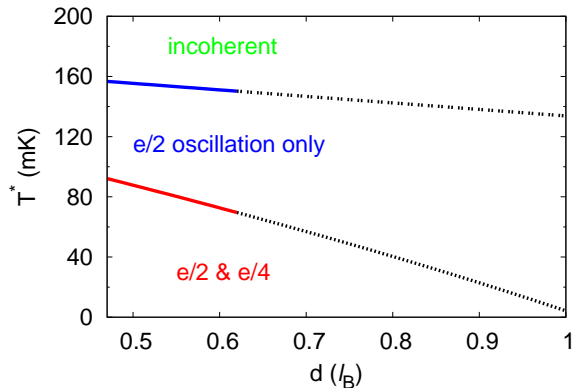


FIG. 4: (color online) Coherence temperature T^* (based on the estimate of v_c and v_n) as a function of d for both $e/4$ (upper line) and $e/2$ (lower line) quasiparticles in the Moore-Read state in an $L = 1 \mu\text{m}$ sample. The broken lines at $d > 0.62l_B$ are obtained by the extrapolation of the velocities, as the Moore-Read state is no longer groundstable in a system of 12 electrons in 26 orbitals. A stripe phase may emerge below $d = l_B$.²⁰

V. DISCUSSION AND CONCLUSION

The narrow range of both charge-mode and neutral-mode velocities, Abelian or not, appears to be surprising, as the velocities are sensitive to confining potential and electron-electron interaction. This is, however, understandable. Despite the stability in the bulk, edges of fractional quantum Hall states are fragile.^{10,12} For $\nu = 5/2$, multiple competing phases also exist in the bulk.^{17,18,20,52,53} Therefore, a significant change of the edge-mode velocities must follow from significant changes of parameters, which normally lead to various instabilities. For example, when background confining potential becomes weaker, edge reconstruction^{10,11,12} takes place, changing the ground state and creating additional neutral modes with smaller velocities. Consequently, v_c increases

in the reconstructed case (see Fig. 10 in Ref. 12). It is, however, possible that v_n can become smaller in the weaker confining potential that leads to edge reconstruction.²¹

In reality, the finite spread of the electron wavefunction in the perpendicular direction tends to soften the Coulomb interaction. While we focus strictly on zero layer thickness in the presentation, the velocity ranges cannot change too much because the finite thickness also changes the confining potential arising from charge neutrality, so the groundstability windows shift accordingly.¹² Perhaps the most uncertain factor is the filled lowest Landau level neglected completely in the calculation for $\nu = 5/2$. However, we expect that the enforcement of the criterion of groundstability is likely to protect the velocities from deviating significantly.

In conclusion, we have calculated the ranges of edge-mode velocities in various FQH states using a microscopic model with long-range interaction and tunable confining potential. In the Moore-Read phase for $\nu = 5/2$, our calculations conclude that the charge-mode velocity is consistently much greater than the neutral-mode velocity, leading to the Bose-Fermi separation and the dominance of $e/2$ and $e/4$ oscillations at different temperature ranges in a quantum Hall interferometer,²⁰ which is consistent with the recent interferometry experiments.^{30,31}

ACKNOWLEDGMENTS

We thank Claudio Chamon and Bas Overbosch for helpful discussion on the measurement of edge-mode velocities. This work was supported in part by NSF grants No. DMR-0704133 (K.Y.) and DMR-0606566 (E.H.R.), as well as PC-SIRT Project No. IRT0754 (X.W.). X.W. acknowledges the Max Planck Society and the Korea Ministry of Education, Science and Technology for the joint support of the Independent Junior Research Group at the Asia Pacific Center for Theoretical Physics.

¹ X. G. Wen, *Int. J. Mod. Phys. B* **6**, 1711 (1992).

² X. G. Wen, *Phys. Rev. B* **41**, 12838 (1990).

³ F. E. Camino, W. Zhou, and V. J. Goldman, *Phys. Rev. B* **74**, 115301 (2006).

⁴ D. T. McClure, Y. Zhang, B. Rosenow, E. M. Levenson-Falk, C. M. Marcus, L. N. Pfeiffer, K. W. West, *Phys. Rev. Lett.* **103**, 206806 (2009).

⁵ M. Grayson, D. C. Tsui, L. N. Pfeiffer, K. W. West, and A. M. Chang, *Phys. Rev. Lett.* **80**, 1062 (1998). Exact Solution for Bulk-Edge Coupling in the Non-Abelian $\nu = 5/2$ Quantum Hall Interferometer

⁶ A. H. MacDonald, *Phys. Rev. Lett.* **64**, 220 (1990).

⁷ C. L. Kane, M. P. A. Fisher, and J. Polchinski, *Phys. Rev. Lett.* **72**, 4129 (1994).

⁸ Z.-X. Hu, H. Chen, K. Yang, E. H. Rezayi, X. Wan, *Phys. Rev. B* **78**, 235315 (2008).

⁹ C. Chamon and X.-G. Wen, *Phys. Rev. B* **49**, 8227 (1994).

¹⁰ X. Wan, K. Yang, and E. H. Rezayi, *Phys. Rev. Lett.* **88**, 056802 (2002).

¹¹ K. Yang, *Phys. Rev. Lett.* **91**, 036802 (2003).

¹² X. Wan, E. H. Rezayi, and K. Yang, *Phys. Rev. B* **68**, 125307 (2003).

¹³ B. J. Overbosch and X.-G. Wen, arXiv:0804.2087 (unpublished).

¹⁴ D.-H. Lee and X.-G. Wen, cond-mat/9809160 (unpublished).

¹⁵ A. Lopez and E. Fradkin, *Phys. Rev. B* **59**, 15 323 (1999).

¹⁶ G. Moore and N. Read, *Nucl. Phys. B* **360**, 362 (1991).

¹⁷ M. Levin, B. I. Halperin, and B. Rosenow, *Phys. Rev. Lett.* **99**, 236806 (2007).

¹⁸ S.-S. Lee, S. Ryu, C. Nayak, and M. P. A. Fisher, *Phys. Rev. Lett.* **99**, 236807 (2007).

¹⁹ X. Wan, K. Yang, and E. H. Rezayi, *Phys. Rev. Lett.* **97**, 256804 (2006).

²⁰ X. Wan, Z.-X. Hu, E. H. Rezayi, and K. Yang, *Phys. Rev. B* **77**, 165316 (2008).

- ²¹ D. Ferraro, A. Braggio, M. Merlo, N. Magnoli, and M. Sassetti, Phys. Rev. Lett. **101**, 166805 (2008).
- ²² C. Chamon, D. E. Freed, S. A. Kivelson, S. L. Sondhi, and X.-G. Wen, Phys. Rev. B **55**, 2331 (1997).
- ²³ E. Fradkin, C. Nayak, A. Tsvelik, and F. Wilczek, Nucl. Phys. B **516**, 704 (1998).
- ²⁴ S. Das Sarma, M. Freedman and C. Nayak, Phys. Rev. Lett. **94**, 166802 (2005).
- ²⁵ A. Stern and B. I. Halperin, Phys. Rev. Lett. **96**, 016802 (2006).
- ²⁶ P. Bonderson, A. Kitaev, and K. Shtengel, Phys. Rev. Lett. **96**, 016803 (2006).
- ²⁷ W. Bishara and C. Nayak, Phys. Rev. B **77**, 165302 (2008).
- ²⁸ H. Chen, Z.-X. Hu, K. Yang, E. H. Rezayi, and X. Wan, arXiv:0905.3607, to appear in Phys. Rev. B.
- ²⁹ W. Bishara, P. Bonderson, C. Nayak, K. Shtengel, and J. K. Slingerland, Phys. Rev. B **80**, 155303 (2009).
- ³⁰ R. L. Willett, L. N. Pfeiffer, and K. W. West, Proc. Natl. Acad. Sci. U.S.A. **106**, 8853 (2009).
- ³¹ R. L. Willett, L. N. Pfeiffer, and K. W. West, arXiv:0911.0345 (unpublished).
- ³² B. Rosenow, B. I. Halperin, S. H. Simon, and A. Stern, Phys. Rev. Lett. **100**, 226803 (2008).
- ³³ B. Rosenow, B. I. Halperin, S. H. Simon, and A. Stern, Phys. Rev. B **80**, 155305 (2009).
- ³⁴ W. Bishara and C. Nayak, Phys. Rev. B **80**, 155304 (2009).
- ³⁵ B. Rosenow and B. I. Halperin, Phys. Rev. Lett. **98**, 106801 (2007).
- ³⁶ S. Ihnatsenka and I. V. Zozoulenko, Phys. Rev. B **77**, 235304 (2008).
- ³⁷ Y. Zhang, D. T. McClure, E. M. Levenson-Falk, C. M. Marcus, L. N. Pfeiffer, and K. W. West, Phys. Rev. B **79**, 241304(R) (2009).
- ³⁸ See, for example, A. H. MacDonald, Phys. Rev. B **30**, 3550 (1984).
- ³⁹ A terminology borrowed from D. Charrier and C. Chamon, Ann. Phys. (2009), doi:10.1016/j.aop.2009.09.004.
- ⁴⁰ For recent progress on ultra-high-mobility GaAs samples, see L. Pfeiffer and K. W. West, Physica E **20**, 57 (2003).
- ⁴¹ See, for example, L. Pfeiffer, K. W. West, H. L. Stormer, and K. W. Baldwin, Appl. Phys. Lett. **55**, 1888 (1989).
- ⁴² The ground state angular momentum for $\nu = 2/3$ depends on both d and N so the scaling analysis is impossible for accessible system sizes. We artificially introduced the finite-size effect (marked by the error bars in Fig. 3) based on the amount observed in the Laughlin case.
- ⁴³ M. D. Johnson and A. H. MacDonald, Phys. Rev. Lett. **67**, 2060 (1991).
- ⁴⁴ M. Milovanović and Th. Jolicœur, arXiv:0812.3764 (unpublished).
- ⁴⁵ R. C. Ashoori, H. L. Stormer, L. N. Pfeiffer, K. W. Baldwin, and K. West, Phys. Rev. B **45**, 3894 (1992).
- ⁴⁶ N. B. Zhitenev, R. J. Haug, K. v. Klitzing, and K. Eberl, Phys. Rev. Lett. **71**, 2292 (1993).
- ⁴⁷ For *unscreened* Coulomb interaction, the charge velocity v_c is expected to diverge logarithmically in the long-wave length limit. Such slow divergence is not visible in our small size studies. In real samples the Coulomb interaction is screened by metallic gates; thus this divergence is cut off and not relevant.
- ⁴⁸ Yue Yu, J. Phys.:Condens. Matter **19**, 621 (2007).
- ⁴⁹ B. J. Overbosch and C. Chamon, Phys. Rev. B **80**, 035319 (2009).
- ⁵⁰ A. Seidel and K. Yang, arXiv:0908.1970 (unpublished).
- ⁵¹ C. Wang and D. E. Feldman, arXiv:0909.3111 (unpublished).
- ⁵² X. G. Wen, Phys. Rev. Lett. **66**, 802 (1991); B. Blok and X. G. Wen, Nucl. Phys. B **374**, 615 (1992).
- ⁵³ B. I. Halperin, Helv. Phys. Acta **56**, 75 (1983).